

## Technical

# Belt edge deterioration in radial steel belted tires

By Uday Karmarkar

Akron Rubber Development Laboratory Inc.

The U.S. Congress passed the Transportation Recall Enhancement, Accountability and Documentation Act in November 2000. The mandate to upgrade tire safety standards to NHTSA resulted in substantial amount of tire research by NHTSA as well as industry bodies such as ASTM. A new tire aging standard requires understanding the aging mechanisms in tires and devising an accelerated laboratory test to match field behavior. With this as the background, we present a new benchmarking technique to rank tire resistance to belt edge deterioration. We present the recent evolution of tire material property testing in the last four years and its applica-

### TECHNICAL NOTEBOOK

Edited by Harold Herzlich

bility to tire aging test development.

Traditional rubber compounds have been studied extensively in the lab using rheometer, tensile tests, Demattia test as well as the good rich flexometer. The study of rubber compound had been limited by the lack of available data from the field. In the recent years, research has been conducted on tire aging phenomena.

NHTSA has published data on tires collected from Phoenix. Thermo-oxidation has been cited as the root mechanism of tire aging. A number of compo-

## Executive Summary

Traditional test methods, such as road wheel endurance testing, high speed road wheel testing, low-inflation road wheel testing, resistance to bead unseating, plunger testing, model compound rheology analysis, short term field testing, etc., are utilized to study and rank expected tire performance in the field. These tests perform a crucial role in ranking tires. However, these tests do not necessarily have the capability to rank tires based on their resistance to belt edge separation in the belt coat compounds generally in use in radial steel belted tires. We present the recent evolution of tire material property testing and its applicability to rank tire aging resistance. An illustrative example will be presented to study the effect of temperature, time, tire cavity oxygen partial pressure and antioxidant level on model compounds oven-aged in tire cavities.

Additionally the aged tires are analyzed using new road wheel test techniques. The mechanism of belt edge deterioration and crack growth development along the edge of radial steel belted tires will be presented using the techniques of "Circumferential Cuts" and "Stepped Shearography" to illustrate its usefulness to evaluate the effect of time, temperature and partial pressure of oxygen as a predictive tool.

Understanding the chemistry changes that occur in a tire over many years is an important factor in devising new tests to evaluate expected field product performance tests. This paper will present these new testing techniques developed by Akron Rubber Development Laboratory Inc. to rank tires based on the aging factors contributing to the belt edge deterioration in radial steel belted tires. This predictive methodology of rubber product change monitoring is a practical guide for ranking tires, benchmarking tire designs and material changes, and other natural rubber applications where product performance and life are affected by crack growth development due to thermo-oxidative aging mechanisms.

ment testing techniques have been used to understand the mechanisms of aging as well as to develop tire durability tests. Materials research plays an important role in tire durability test development. Specifically our paper focuses on the stepped shearography technique to evaluate the belt edge crack growth develop-

ment in tires as well as circumferential technique to understand the complex nature of crack growth at the belt edges.

We also present in our paper materials research on aging of belt coat compounds and the effect of time, temperature and antioxidant and partial pressure of oxygen on compound development. The com-

pound that we studied was natural rubber that is used between the steel belts of radial tires. A number of test methods were developed to study the chemistry changes in the rubber with aging as well as with the fatigue crack growth changes due to thermo-mechanical effects taking place during the field usage of a tire.

Material and structural tests, such as tensile, mini Demattia, high speed peel, proton NMR, slip and camber, innerliner permeation and crosslink chemistry are used to guide this test development work. Model compounds also were studied using a novel design of experiment technique.

This study aims to develop a methodology to study tire behavior in a design box of varying external factors. Improved tire compounding and design are the internal factors that have been kept constant in this study and will influence the tire rank in this benchmarking practice. The external factors that influence tire belt edge deterioration are time, temperature and tire cavity partial pressure of oxygen.

### Experimental

#### Design of experiments

A statistical design of experiments was set up using JMP Statistical Discovery Software Release: 5.0.1.2. Four inputs were studied, temperature, time, partial pressure of oxygen, antioxidant level. A full factorial 2x2x2x2 design of experiments was set up with a single center point. The data from the experiments is plugged into the same JMP program to handle and model the inputs with the output generated and illustrate the influence of the effects on the output.

The design of experiment conditions of inputs are maintained using calculated pressures and adjusted based on temperatures to maintain the same level of partial pressure of oxygen levels at all the design points.

This novel design of experiment provides us with two studies with a minimal usage of materials and time. The first study is the effect of the four inputs on the compounded slabs aging inside the tire reactors. The second study is the effect of time, temperature and partial pressure of oxygen on the tires used as reactors.

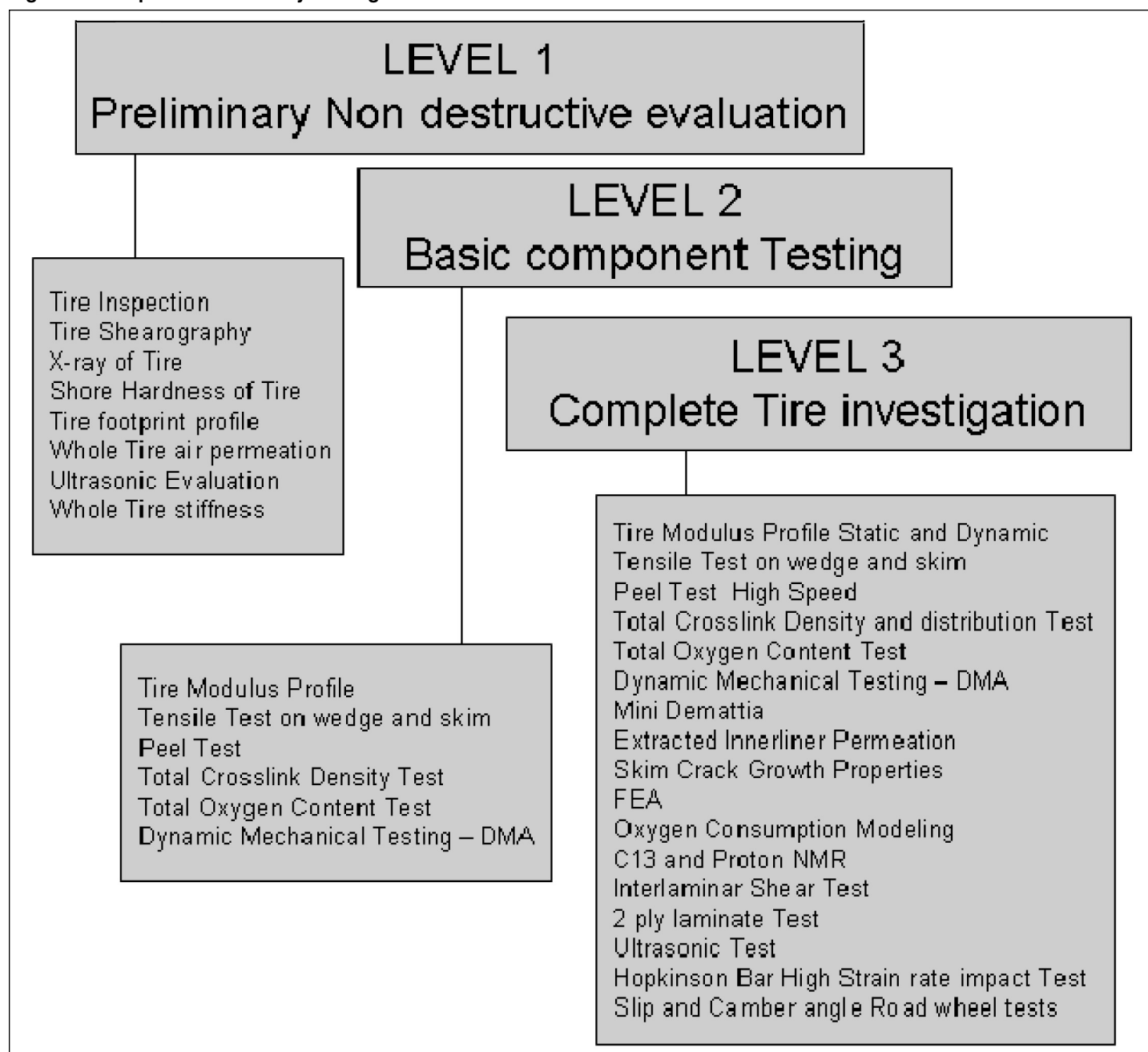
#### Nitrogen/oxygen ratio

The compounded slabs were aged in the inner cavity of the tire. This allows for the accurate measurement and monitoring of the partial pressure of the oxygen in the vicinity of the samples as well as accurate aging of the tire reactors in calibrated ovens for different times. The partial pressure was maintained within 5 percent of the original set value. Tires were flushed and refilled to adjust to the original partial pressure of oxygen value. This compensates for the loss of the cavity gas due to whole tire permeation.

The design box encompasses real world conditions. If a tire is filled to 80 psi, the resulting partial pressure of oxygen is 19.79 psia. The nitrogen-oxygen ratio is an important factor in this study. For a tire with a target pressure of 32 psig, filling with a nitrogen generator of 98-percent nitrogen purity output will generate a final nitrogen purity of 92, 96 and 97 percent with each successive complete refill.

Similarly, for a nitrogen generator of 95 percent purity output, we achieve 90-, 94- and 95-percent target purity with each successive complete refill. It has

Fig. 1. Techniques used to study NR degradation mechanisms in tires.



## Technical

been shown that property changes with greater than 95 percent purity in a tire are within the error limits inherent in tire cure variations. Consequently our study indicates a practical minimum level of 95 percent purity of nitrogen is desirable.

### Materials

#### Compounded materials

Three types of compounds were formulated based on typical belt coat compounds used in tires. The three compounds are designated by letters A, B and C differentiating the level of antioxidants used 0.5, 1.25 and 2 phr. The formula is shown in **Fig. 2**. All slabs are compression molded to a uniform thickness of 40/1000th of an inch.

#### Tire reactors

Five tire reactors were used. All five tire reactors were of one size and DOT code LT245/75R16 load range E, rated load of 3042 pounds at 80 psi cold with

two steel, two polyester and two nylon plies in the tread. Two types of materials were evaluated. A design of experiment was set up to illustrate the effect of the four inputs on two types of materials.

The design of experiments set up resulted in two superimposed studies. The first is the effect of time, temperature, partial pressure of oxygen and antioxidant level on compounded material properties aged in tire reactors. The second is the effect of time, temperature and partial pressure of oxygen on the tire manufactured with an unchanged chemical formulation. For the first study, compounded rubber slabs are aged in specially marked polyethylene bags inside the tire reactors. Tensile specimens are punched out and three samples are aged for each design of experiment condition. Additionally, intact rubber slabs are aged to avoid severe diffusion limited oxidation conditions. Four tires also were aged to complete the design box for the

**Fig. 2. Formulation used to study model belt coat compound.**

Ingredient	Supplier Code	Description	phr
<b>Non-productive mix</b>			
Natural Rubber			100
Carbon Black N326			65
Aromatic Oil			3
ZnO			5
Stearic Acid			2
Cobalt Naphthenate	Manobond 680C		0.5
TMQ			1
<b>Productive mix</b>			
ZnO			3
6PPD			formula A = .5 formula B = 1.25 formula C = 2
Santogard PVI			0.1
Insoluble sulfur	crystex sulfur	80% sulfur	5.6
DCBS			0.7
<b>Total</b>			<b>formula A = 185.50 formula B = 186.25 formula C = 187.00</b>

**Fig. 3. Correlations with one center point to construct formulation among time, temperature, antioxidant level and partial pressure of oxygen.**

2x2x2x2 Factorial		Pattern	Temp. (Celcius)	Part. Press. O2 (psia)	Antioxidant level (phr)	Time (days)	Elongation to break (percent)
Design	2x2x2x2 Factorial	1 ----	50	1	0.5	7	550.26
Model		2 +++-	70	21	2	7	490.16
		3 ++++	70	21	0.5	49	157.22
		4 +-+-	70	1	2	7	516.66
		5 +++	70	1	2	49	339.11
		6 ++++	70	21	2	49	179.27
		7 ---+	50	1	0.5	49	556.3
		8 -+++	50	21	2	49	526.9
		9 ---+	50	1	2	49	573.36
		10 -+-	50	21	0.5	7	541.47
		11 +--+	70	1	0.5	49	323.1
		12 ++--	70	21	0.5	7	456.56
		13 +---	70	1	0.5	7	481.36
		14 -++-	50	21	2	7	561.68
		15 0000	60	11	1.25	28	481.1
		16 --+-	50	1	2	7	590.42
		17 -++	50	21	0.5	49	496.06

### The author

Uday Prakash Karmarkar is a business development manager for Akron Rubber Development Laboratory Inc. Karmarkar worked as staff engineer prior to his current assignment at ARDL. Karmarkar has been active in new test development and aging research in tires. He has published more than 10 scientific articles and presentations on the subject of tires, automotive, aerospace, medical products and predictive materials research. Karmarkar has a bachelor's degree in chemical engineering and a master's from the College of Polymer Engineering and Polymer Science at the University of Akron. He published a thesis on aircraft composite design optimization at the University of Akron before joining ARDL.

tire crack growth study.

#### Fill gas

Nitrogen and oxygen fill gas tanks are obtained from Praxair. The gases obtained are dry and contain less than 10 ppm of moisture. The gas is mixed to achieve the required percent of oxygen in the tire reactors based on the design of experiments.

#### Physical properties

##### Oxygen content

Oxygen content of the tire reactors was measured using a Balston 72-730 Oxygen Analyzer from Parker Hannifin Corp. The Balston 72-730 Oxygen Analyzer is designed to monitor the oxygen concentration in a process stream and display this concentration in digital form. The Balston oxygen analyzer has been certified to IEC 1010 Standards (CSA 22.2 No.1010.1-92) and bears the CSA safety marking on the product label.

The sensing device designed into the Balston 72-730 and 72-O2730NA oxygen analyzers is a galvanic cell. The oxygen analyzer has an internal temperature compensation circuit to provide accurate readings within a specified temperature range, with an accuracy of  $\pm 1$  percent of the calibration gas concentration. The oxygen concentration LED display shows oxygen concentration, in percent, to the nearest 0.1 percent. The calibration controls are located to the left of the oxygen concentration display. The zero potentiometer is used to zero the instrument when a zero gas (containing no oxygen) is introduced.

#### Tire pressure

Tire pressure measurement is done

using a digital pressure gauge with a range of 0-100 psig with pressure resolution of 0.5 psig. The tire pressure gauge is calibrated traceable to a NIST calibration certificate.

#### Temperature humidity measurements

Oven aging is calibrated with a NIST traceable Humidity Temperature Meter from Omega with add-on K type thermocouple.

#### Tensile testing

Dumbbell specimens were die-cut using an ASTM D 638 Type V dumbbell die and tested per ASTM D 412. Samples were tested at 2.0 inches per minute (50.08 cm/minute). Testing was done in a controlled environmental space maintained at 50-percent relative humidity and at 70°F. Test output includes elongation to break, stress at break, modulus at 25 percent, 50 percent, 100 percent, 200 percent, 300 percent and 400 percent elongation.

#### Road wheel FMVSS testing

The tires reactors were tested according to FMVSS 139 stepped up load endurance test conditions.

#### Stepped shearography

Shearography evaluation was conducted using an ITT compact SDS Laser Interferometry Equipment. Testing was conducted at 50 millibars. The defect sizes were calibrated using a calibration block. ARDL stepped shearographic test technique was conducted at a specific angle.

#### Circumferential cut analysis

This test technique is used to expose the rubber at the belt edges between the steel belts in a radial steel belted tire. The tire sections are manually cut with sharp blades to expose the scarring at the belt edges. The defect sizes are measured with the help of a transparent grid overlay on the physical sample and the total of the defect sizes are visually added up and plotted for analysis.

### Results and discussion

As stated in the introduction, we studied the effect of external factors such as time, temperature and cavity gas partial pressure of oxygen on the belt edge crack growth rates for a given radial steel belted tire. **Fig. 1** shows the variety of techniques currently utilized to study the natural rubber degradation mechanisms in tires.

We specifically focused on analyzing the formation of belt edge crack growth initiation and propagation morphologies using the "Circumferential Cuts" and "Stepped Shearography" approach to predict remaining belt edge life in tires.

A model compound study was performed to study the significance of four factors on the rubber tensile property. **Fig. 2** shows the formulation used to study model belt coat compound.

Three levels of antioxidants are compounded and 40/1000th of an inch thick  
See **Belt**, page 14

# Technical

## Belt

Continued from page 13

slabs are molded to avoid diffusion limited oxidation conditions during aging. The rubber model compound is aged in the cavity of tires. Seventeen aging conditions result from nine such tire reactors. Fig. 3 shows the correlations using a 2x2x2x2x full factorial model with one center point to construct a formulation between time, temperature, antioxidant level and partial pressure of oxygen. All four input effects are significant in the elongation to break model.

Fig. 4 indicates the use of a prediction profiler used to maximize the output variable, in this case elongation to break. The JMP program indicates that the significant controlling inputs

are temperature, time and partial pressure of oxygen followed by antioxidant level. It is important to note this conclusion for compound and tire designers. Tire design as well as usage can significantly affect running temperatures. A lower belt temperature can cause less degradation of the rubber compared to a better compounded belt coat compound in the limits of our study variables.

Also, expensive antioxidant amounts get consumed at a quicker pace in the presence of higher partial pressure of oxygen. Inclusion of modulus at 100-percent elongation in the model illustrates that the DLO—Diffusion Limited Conditions—affected the model input of modulus.

Fig. 5 indicates the Ahagon chart analysis method for the tensile test data. This chart shows the plot of the log of the elongation ratio at break on the

Fig. 5. The Ahagon chart analysis method for the tensile test data.

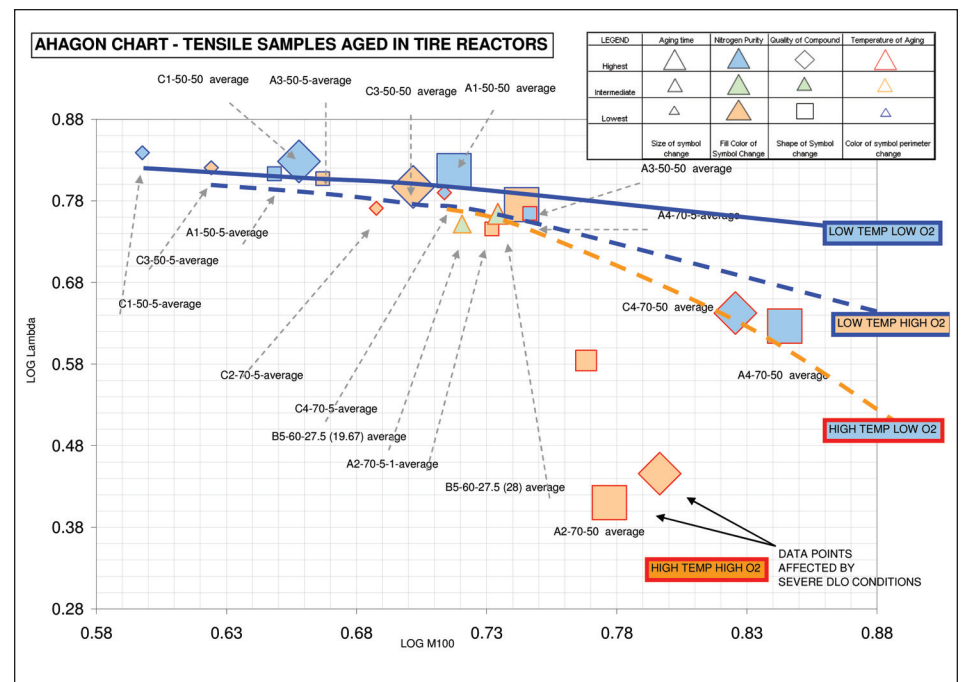


Fig. 7. Design of experiment setup to study the belt edge crack growth effects in tires.

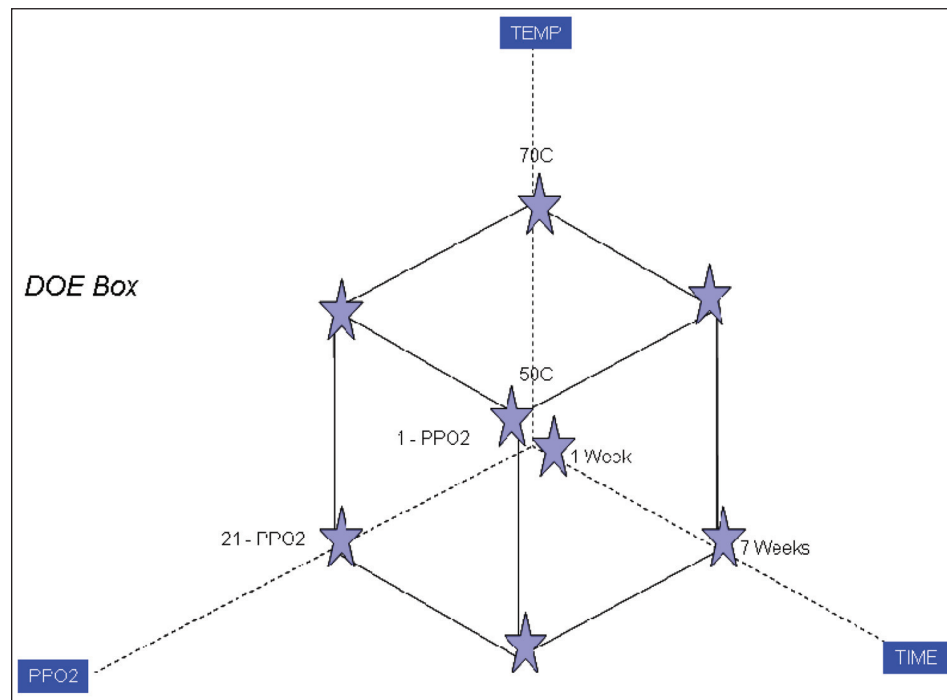


Fig. 4. The use of a prediction profiler used to maximize output variable, elongation to break.

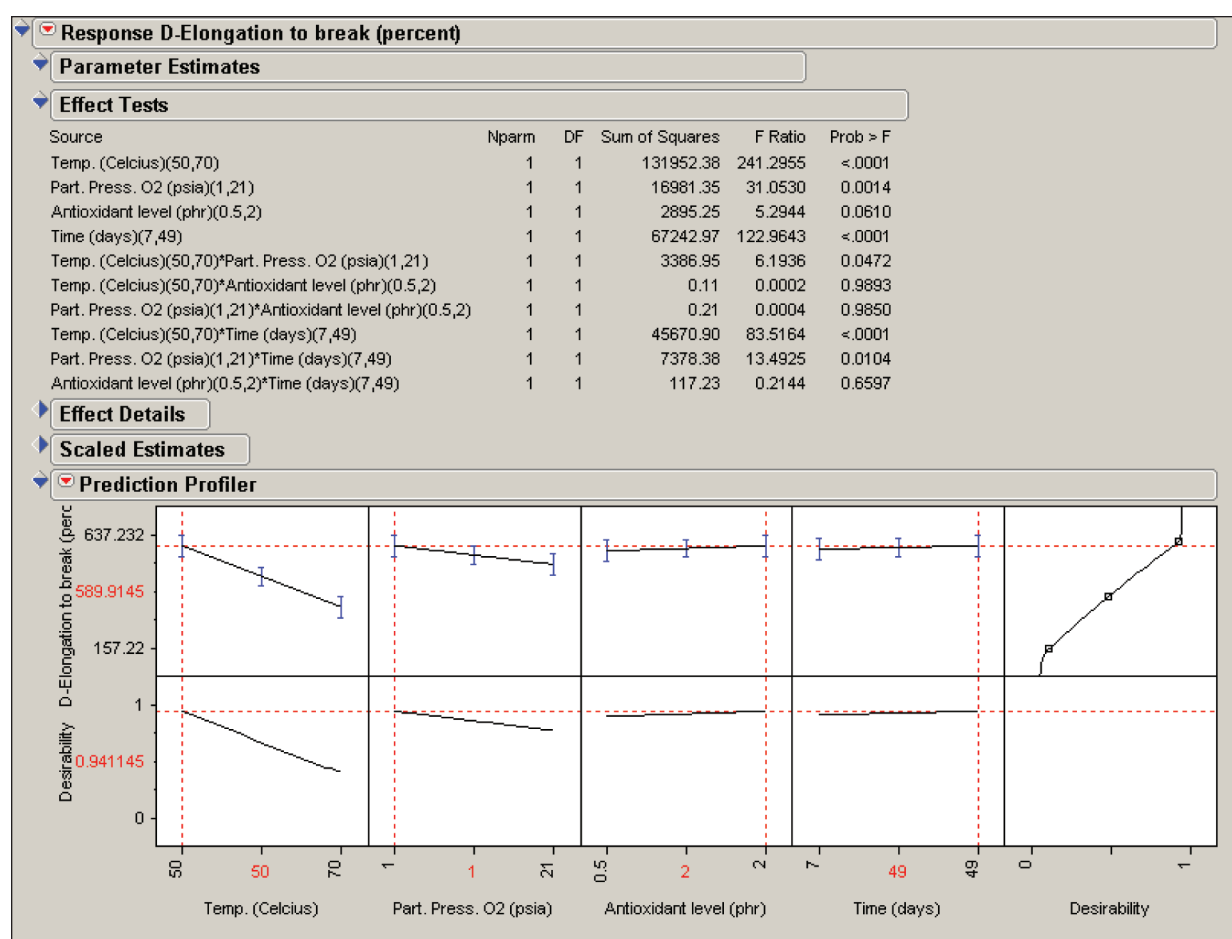
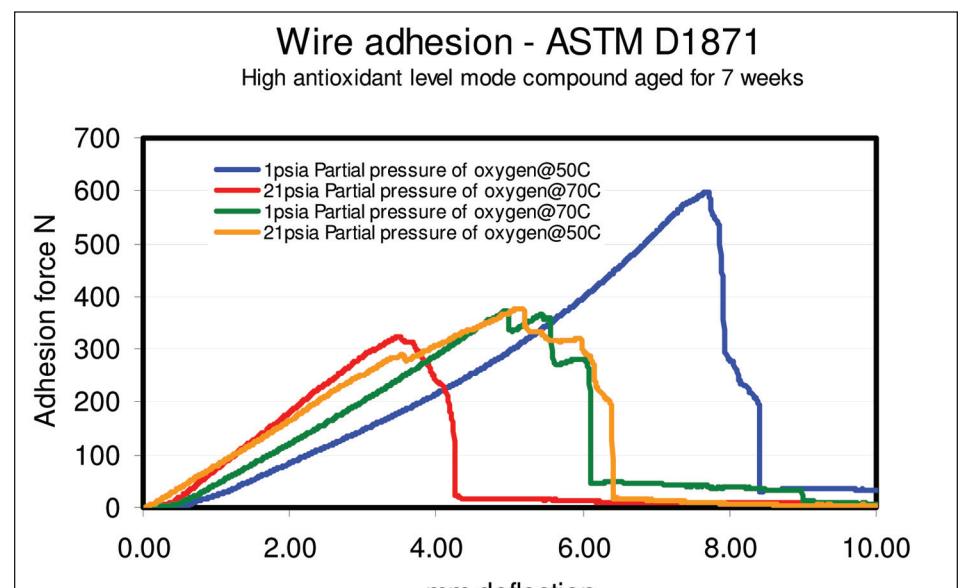


Fig. 6. Wire adhesion pulls on model compounded aged at different temperatures and in varying nitrogen oxygen ratios.



y axis and log of the modulus at 100-percent strain for tensile dumbbells punched out and aged in tire reactors according to the design of experiments. The design of experiments was constructed to illustrate the effect the four input variables had on the rubber properties. We observe a -6 slope for the compounds aged at high temperature and high partial pressure of oxygen irrespective of the quality of the compound.

It is important to note that literature reveals a -0.75 slope for samples aged at a much lower window of partial pressure of oxygen designated by Type I oxidative reactions. However, in our study we aged tensile dumbbells. This affects the data points at high temperature and high partial pressure. A condition of high modulus at the surface due to diffusion limited oxidation exists.

Preliminary testing on the Modulus Profiler indicates a worst-case condition with a factor of three modulus increase between the surface and the inner regions on the slab for the compound with lowest antioxidant aged for the longest time at the highest temperature. This would cause the data point to slide to the right of the chart falling on the -0.75 slope Type I oxidative curve.

It is important to note that the lower purity nitrogen data points would lie farther down this degradation slope. As the surface modulus controls the elongation to break, our model is not affected. It is important to note that we need to understand better the changes in compounded slab studies as we see this effect in slabs that are only 40/1000th of an inch in thickness.

Additionally, wire adhesion samples prepared and aged with the model compound in the tire reactor are tested for wire adhesion strength.

Fig. 6 shows the wire adhesion pulls on model compounded aged at different temperatures and in varying nitrogen oxygen ratios. The effect of the nitrogen oxygen ratio as well as temperature is significant. The lower the

See Belt, page 16

# Belt

Continued from page 14

temperature and the lower the oxygen percent, the higher the wire adhesion to the rubber becomes. Nine tire reactors used for the model compound study are then tested using stepped shearography.

**Fig. 7** shows the design of experiment setup to study the belt edge crack growth effects in tires. Time, temperature and cavity gas oxygen partial pressure are the three external factors of influence. This design box has one center point tire aged for four weeks at 60°C not seen in the figure. The tires are run on a 67-inch endurance test machine and stopped after 10, 22, 34, 38 and 42 hours into the test, and belt edge crack progression is measured.

**Fig. 8** shows the stepped shearography machine used to non-destructively test the belt edge deterioration. Each 360° scan is split into nine sections or sectors as shown.

**Fig. 9** shows the tire cross section cut to illustrate with shaded schematics illustrating the morphology of the belt edge crack growth. The belt edge crack area is estimated based on shearography results.

**Fig. 10** shows the stepped shearography result displayed as a sequence of nine sector scans for one of the nine aged tires. This tire was aged at 60°C for four weeks and endurance tested on a stepped up road wheel test for 10 hours. We do not observe any belt edge

defect formation based on these results.

**Fig. 11** shows the same tire at a time slice of 22 hours. We still do not observe any belt edge defect formation based on these results.

**Fig. 12** shows the same tire at a time slice of 34 hours. Here we observe the belt edges to form dimples as a result of the formation of circumferential crack growth along the edge of the two belts.

**Fig. 13** shows the results at 38 hours. We observe further growth of these belt edge defects now observed as fringe patterns. **Fig. 14** indicates the rise in belt edge defects at 42 hours. We

## Technical

observe now a significant growth of belt edge fringes at the 42 hour mark. This is the end of the second four-hour 10-percent load increment above 34-hour, 100-percent rated load step level.

**Fig. 15** displays the most significant sectors from each of the nine tire reactors at different time splices in the endurance test. The external factors influencing the belt edge deterioration are time, temperature and cavity gas partial pressure of oxygen. The tires are tested on a 67-inch road wheel using the stepped up load endurance test. The nine sectors are displayed in the figure and arranged to reveal the effects of the different factors on the belt edge crack growth. This figure shows the belt edge shearography growth 22 hours into the test.

See Belt, page 18

**Fig. 8. Stepped shearography machine used to non-destructively test the belt edge deterioration.**

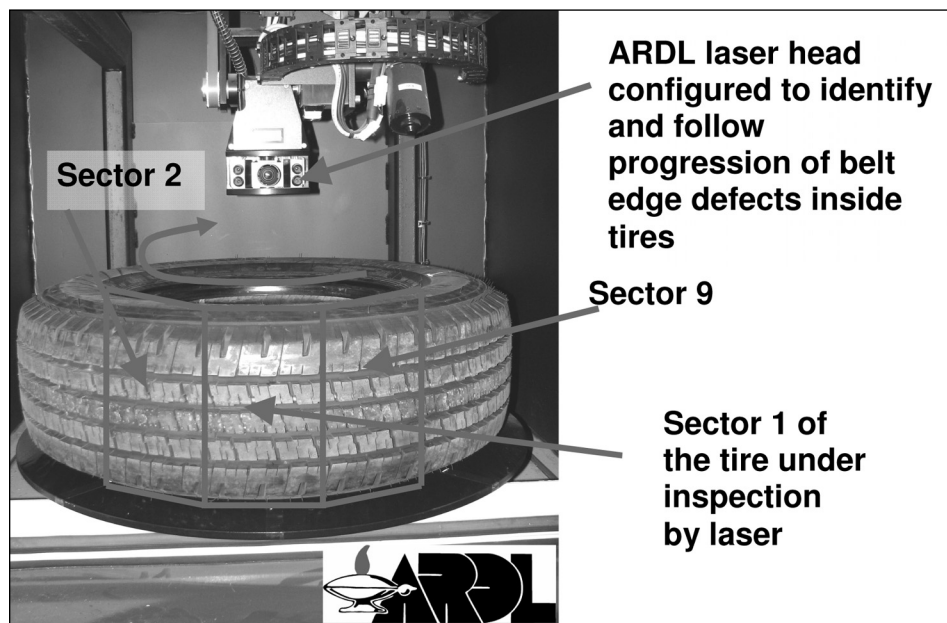


**Fig. 9. Tire cross section cut to illustrate with shaded schematics the morphology of the belt edge crack growth.**

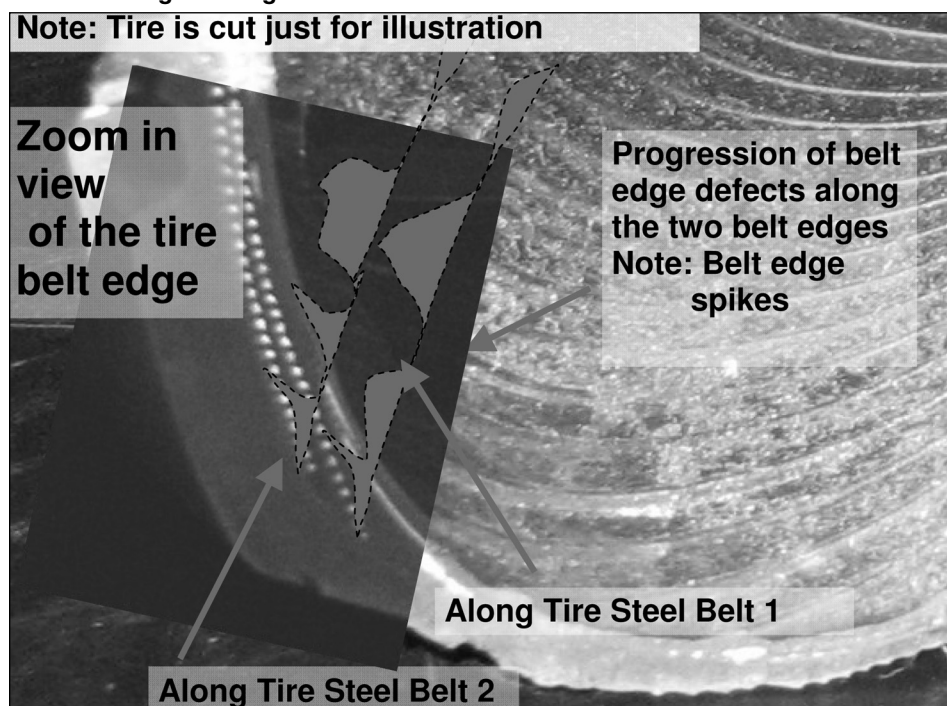


**Fig. 10. Tire aged at 60°C for four weeks and endurance tested for 10 hours.**

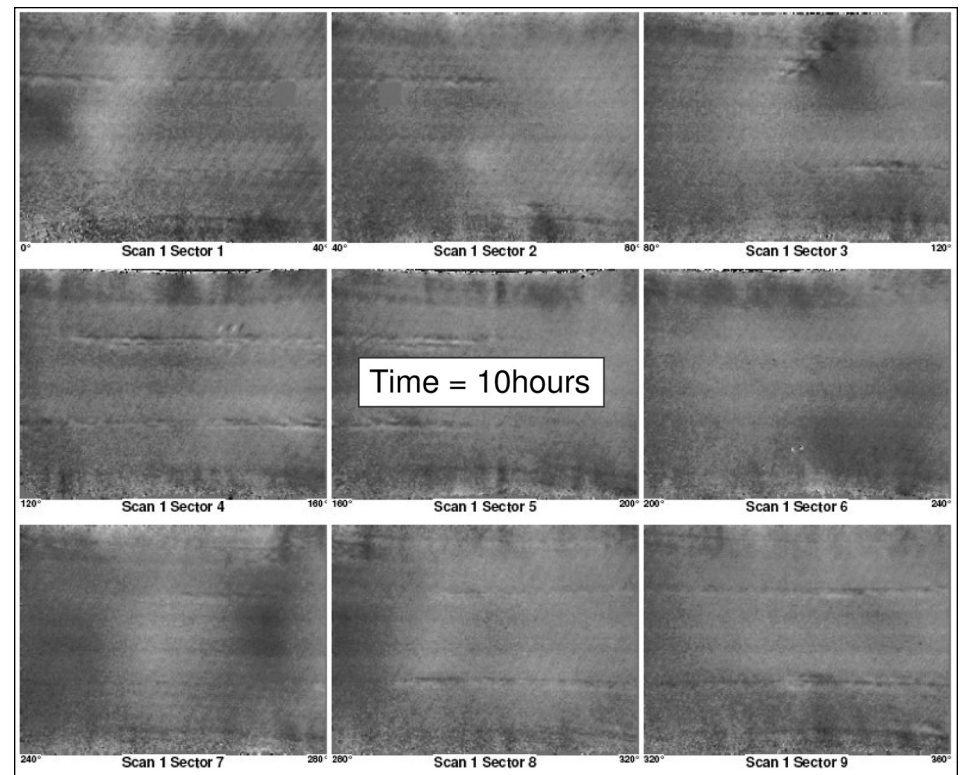


**Fig. 11. Same tire as Fig. 10 at 22 hours.**

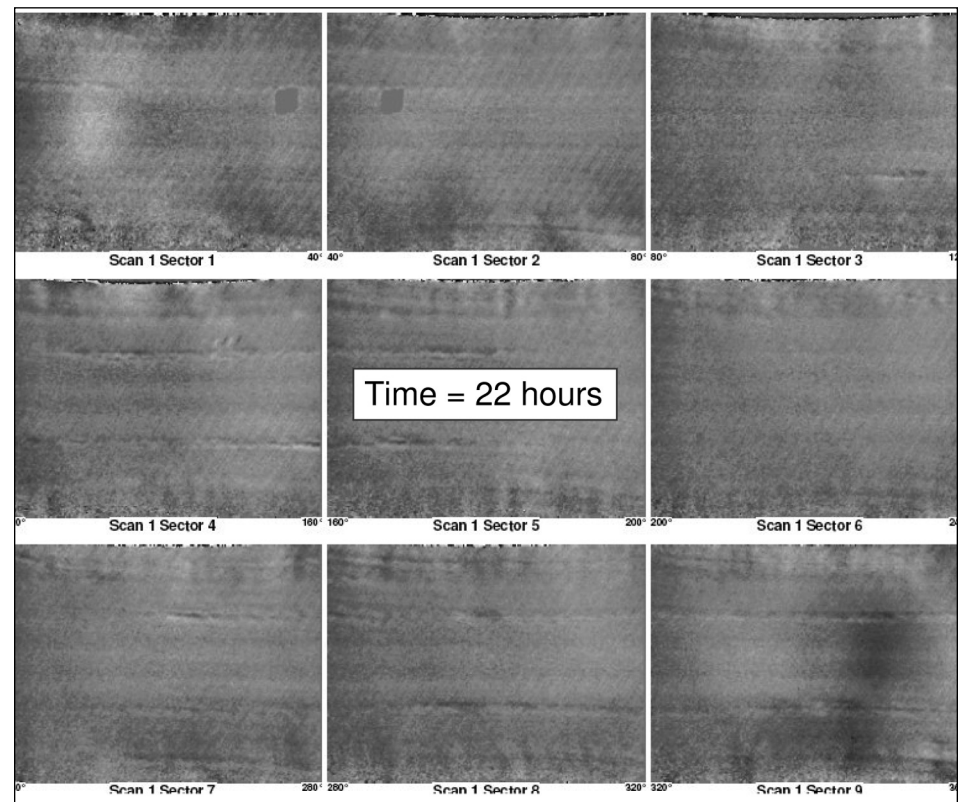
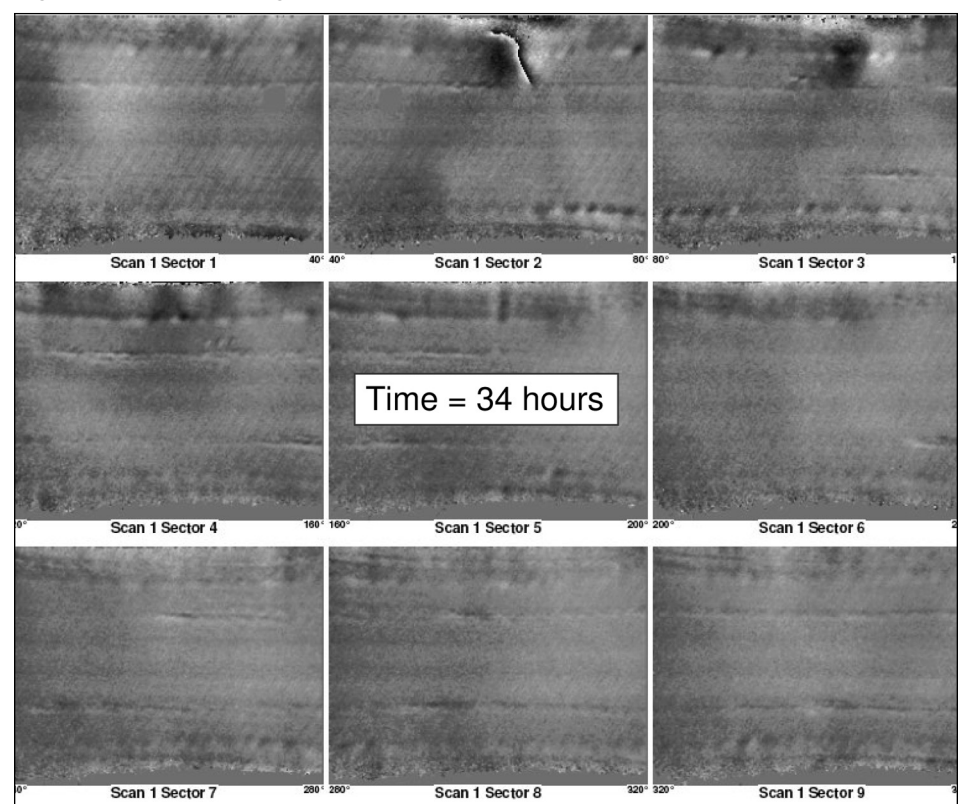


**Fig. 12. Same tire as Fig. 10 at 34 hours.**



## Technical

# Belt

Continued from page 16

**Fig. 16** shows the belt edge shearography growth 34 hours into the test for all nine reactors. **Fig. 17** shows the belt edge shearography growth 38 hours into the test for all nine reactors.

**Fig. 18** shows the belt edge shearography growth 42 hours into the test for all nine reactors. One week aged tires at higher load steps generate uncorrelatable belt edge effects. Aged tires at four and seven weeks show a large reduction in belt edge defects for tires aged at lower temperatures and lower partial pressure of oxygen.

**Fig. 19** shows the crack growth development differences between high-temperature and low-temperature aged tires plotted from the results of shearography belt edge separation defect sizes from the stepped shearography approach.

**Fig. 20** shows data plotted for all the

nine reactors. All the shearographic fringe area data is plotted on a time and millimeters-squared scale to illustrate the nine tire reactors aged at different times, temperatures and partial pressures of oxygen.

However the shearography technique does not correlate to actual defect sizes due to the complex structural nature of the belt edge crack growth. To calibrate and remove this source of error as well as to understand the morphology of the crack growth process, we use the technique of "circumferential cuts" to expose the edge of the belt package.

**Fig. 21** is a schematic cross-section of a radial steel belted tire. The tire closest to the innerliner is called belt No. 1 and the belt closest to the tread is called steel belt No. 2. The red shaded areas are belt edge defects growing toward the center of the tire in a characteristically spiked manner. The edges formed by the steel belts initiate the crack growth development and the rubber thermo-oxidative degradation influences the propagation of these defects.

**Fig. 13.** Same tire as Fig. 10 at 38 hours.

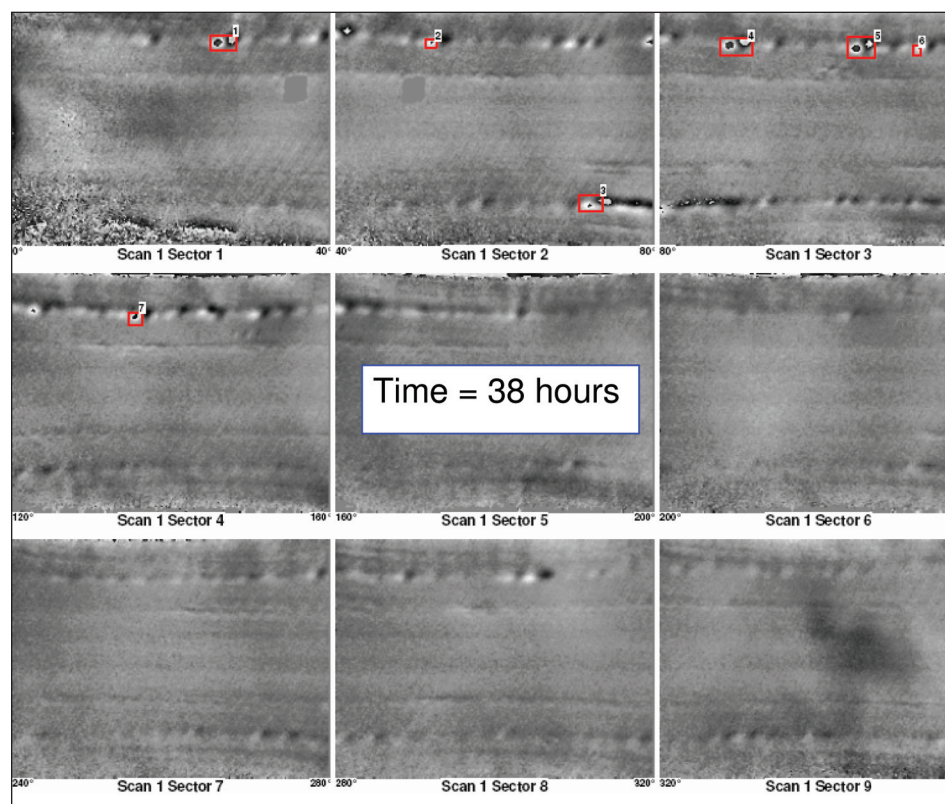


**Fig. 14.** Same tire as Fig. 10 at 42 hours.

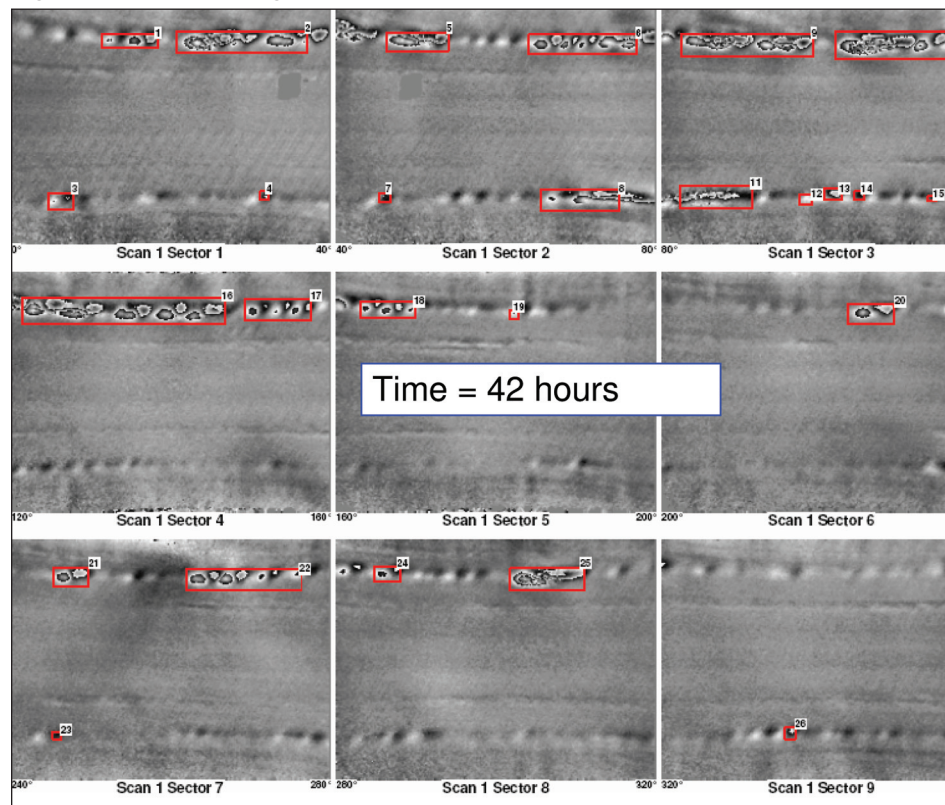


**Fig. 15.** Most significant sectors from each of the nine tire reactors at different time splices in the endurance test, shown here at 22 hours.

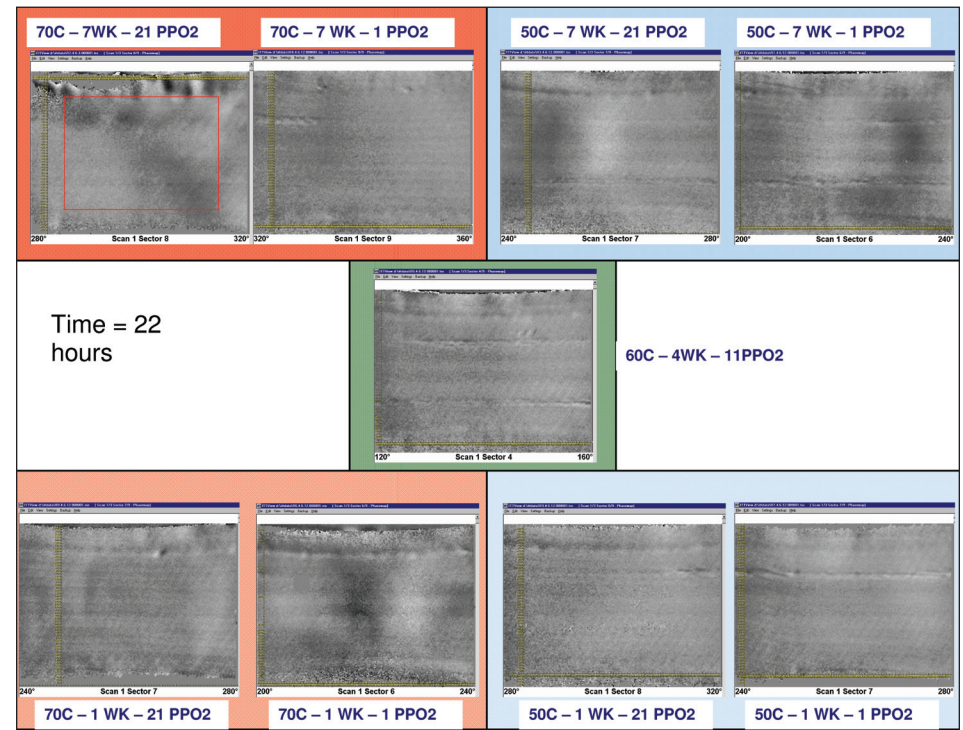


**Fig. 16.** Belt edge shearography growth 34 hours into test for all nine reactors.

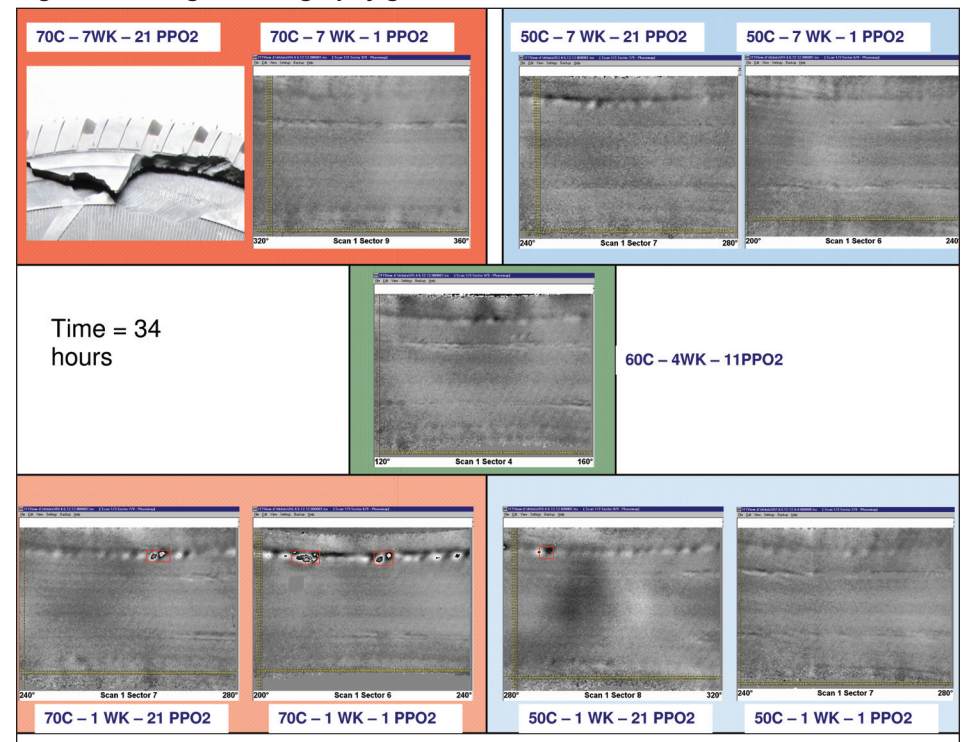
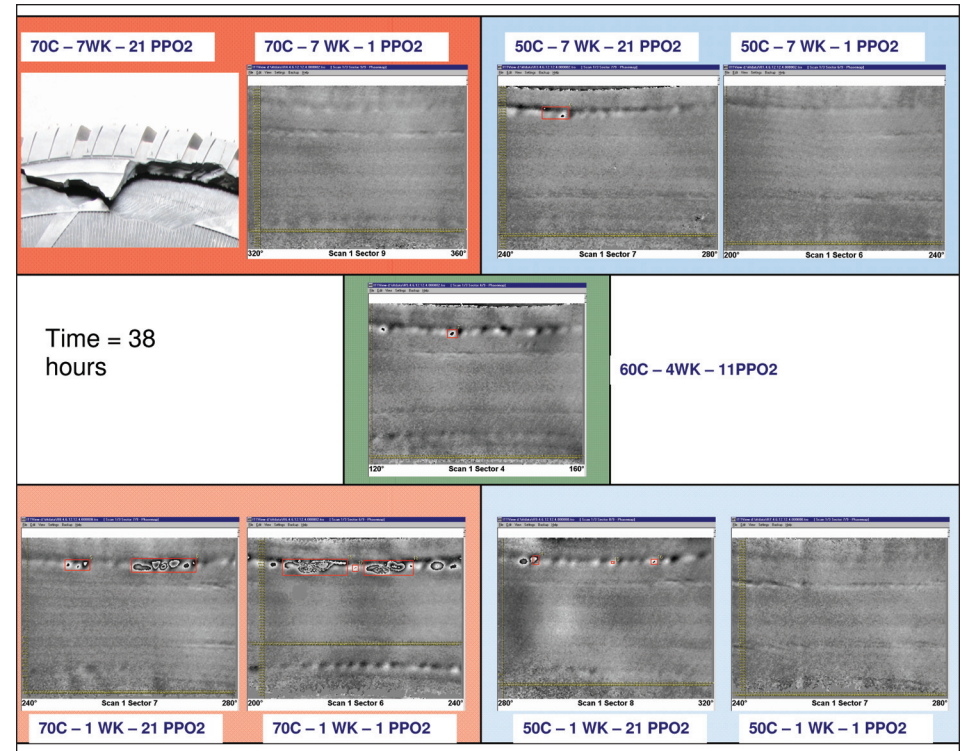


**Fig. 17.** Belt edge shearography growth at 38 hours into test for all nine reactors.



# Technical

**Fig. 22** shows the “circumferential cut” of a tire with the top region of the tire exposed to reveal the scarring at the belt edge two contained in the area enclosed by the two schematically drawn white border lines. The total area is added up using a hand overlay of a transparent grid to measure the actual defect area generated at time slices along the progression of the stepped-up load test. This adjusted data is now plotted as a percent of the total area remaining.

**Fig. 23** shows the corrected plot with actual defect sizes calibrated to the shearography sizes. The y axis is plotted as a percent of the actual available area for complete separation. This provides us with a predictive tool to evaluate the expected tire aging performance in the field. Failure at 80-percent loss of belt integrity can be predicted with a high level of accuracy based on the stepped-up approach.

## Conclusion

The overall conclusion of this study is as follows:

Tire component testing performs an important role in the development of tire aging and durability experiments.

Materials research is a key ingredient in tire test development.

Good benchmarking practice has been developed to study the effectiveness of tires to resist belt edge deterioration.

A good benchmarking technique for tires must encompass and rank tires based on tire response matrix to a design matrix of all three external factors.

We have established the belt edge crack growth mechanisms and morphology of laboratory and road wheel tested tires.

Time (field age), temperature (tire design and usage) and cavity gas partial pressure of oxygen (nitrogen purity in tire) are the critical external factors influencing the belt edge deterioration.

## References

“Aging of Tire Parts during service I Types of aging in heavy-duty tire,” Asahiro Ahagon, M. Kida, and H. Kaidou, presented at a meeting of the Rubber Division, ACS, May 1990.  
 “Aging of Tire Parts during service II Aging of Belt-

skim rubbers in passenger tires,” Hiroyuki Kaidou and A. Ahagon, presented at a meeting of the Rubber Division, ACS, May 1990.

Uday Karmarkar, Harold Herzlich. “Effect of nitrogen purity on the oxidation of belt coat compound,” International Tire Exhibition and Conference 2006, Akron.

NHTSA tire aging docket -NHTSA-2005-21276, <http://dms.dot.gov/>.

K.T.Gillen, R.L.Clough, and J.Wise, “Prediction of Elastomer Lifetimes from Accelerated Thermal Aging Experiments,” ACS, 1996, pp557-575.

G.J. van Amerongen, Rubber Chem Technol. 1065 (1964).

“Long Term Durability of Tires,” N. Tokita, W.D. Sigworth, G.H.Nybakken, G.B.Cuyang, Uniroyal Inc. Research Center, International Rubber Conference, Kyoto, Japan, October 1985.

J. Baldwin, “Effects of Nitrogen Inflation on Tire Aging and performance,” ACS Rubber Division 2004.

“Evaluation of chain scission during mixing of filled compounds,” Asahiro Ahagon.

“Oxidative aging of back filled elastomers,” A. Ahagon, Hiratsuka, presented at a meeting of the Rubber Division, ACS, October 1984

“Property changes in automotive tyre components in road service,” A. Ahagon, International Polymer Science and Technology, Vol. 27, No. 3, 2000.

“Oxidative aging of reinforced elastomers,” L. Nasdala Universitat Hannover, Germany.

“FEA of diffusion -reaction in tires,” Norman Welson, Stevens institute of tech, Rubber World, October 1993.

“The chain end distributions and crosslink characteristics in black filled rubbers,” Asahiro Ahagon.

D.M. Coddington, Rubber Chem Technology. 52, 905 (1979).

**Fig. 18.** Belt edge shearography growth 42 hours into test for all nine reactors.

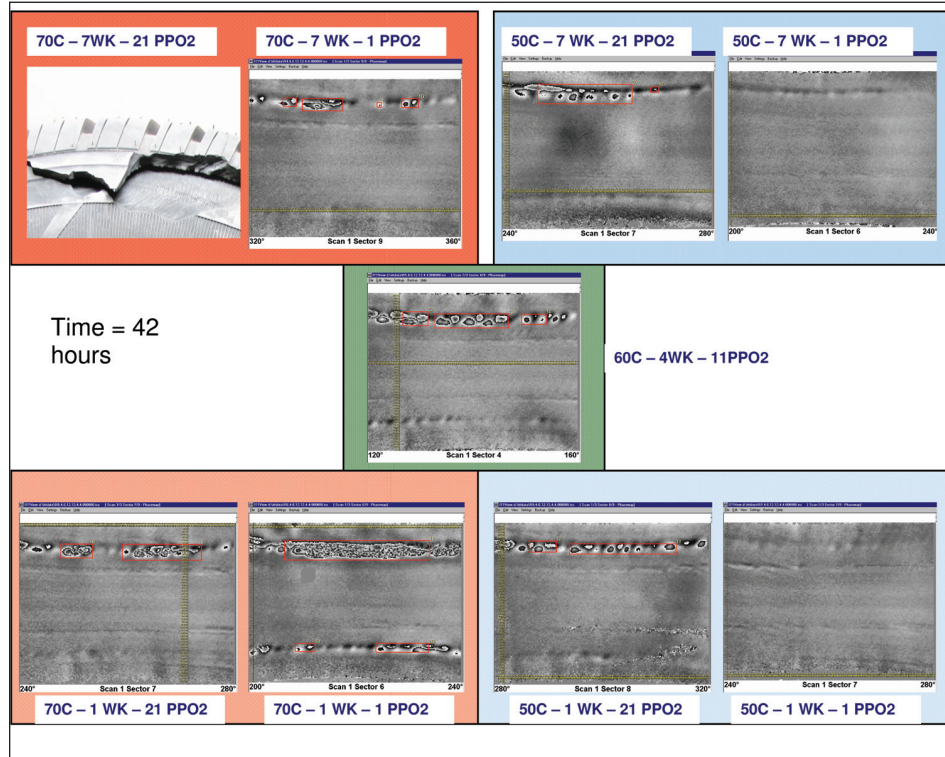


**Fig. 19.** Crack growth development differences between high-temperature and low-temperature aged tires plotted from the results of shearography belt edge separation defect sizes from stepped shearography approach.

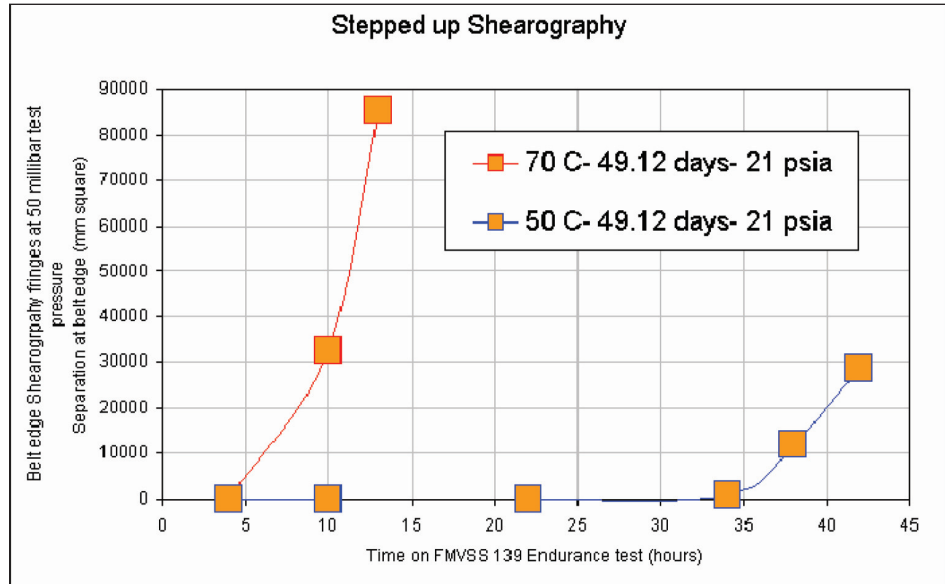


**Fig. 20.** Data plotted for all nine reactors.

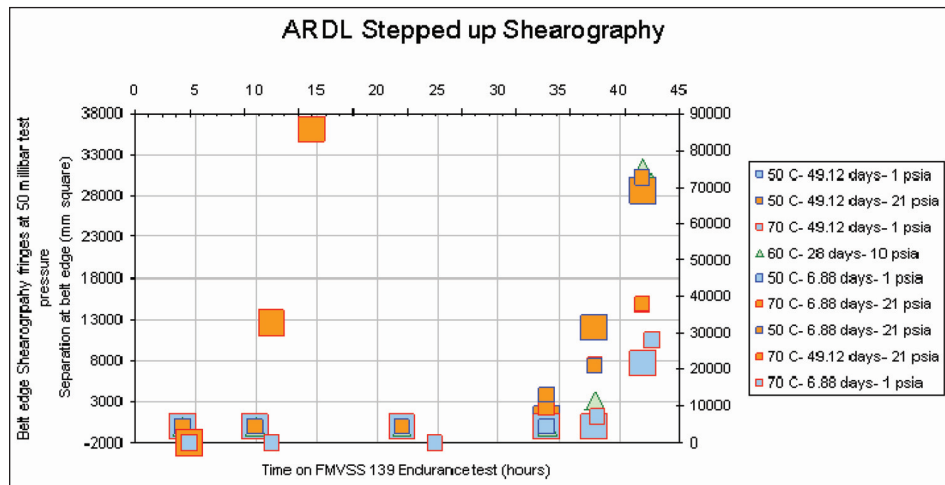


**Fig. 21.** Schematic cross section of a radial steel-belted tire.

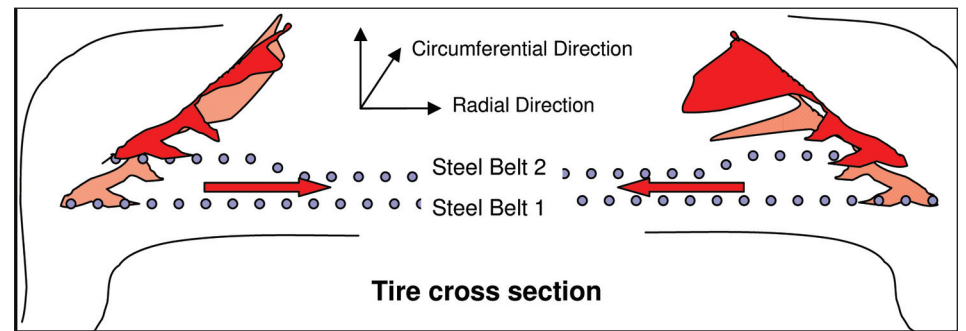


**Fig. 22.** Circumferential cut of a tire with the top region of the tire exposed to reveal the scarring at the belt edge contained in the area enclosed by the two schematically drawn white border lines.

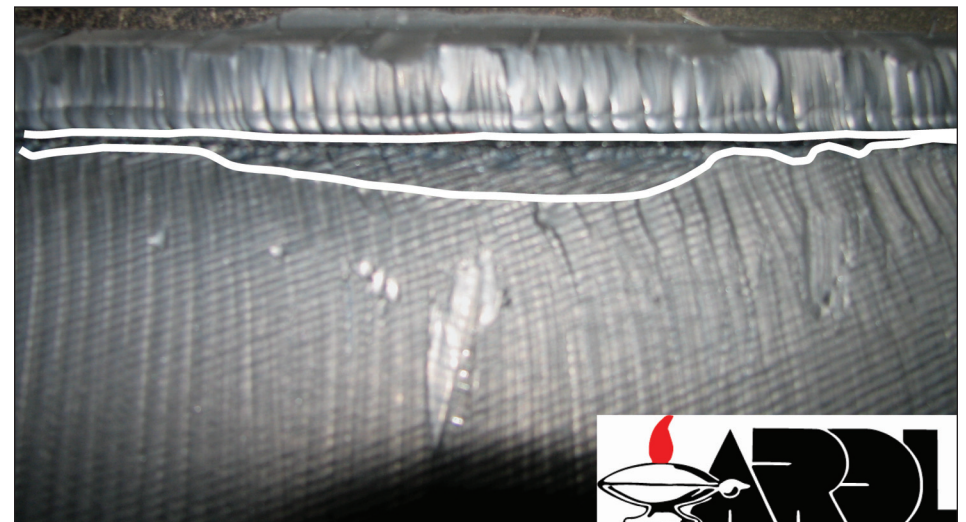


**Fig. 23.** Corrected plot with actual defect sizes calibrated to the shearography sizes.

